COMMUNICATION

Protein film electrochemical EPR spectroscopy as a technique to investigate redox reactions in biomolecules

Received 00th January 20xx,
Accepted 00th January 20xx

DOI: 10.1039/x0xx00000x

Kaltum Abdiaziz,[1] Enrico Salvadori,[1,2] Katarzyna P. Sokol,[3] Erwin Reisner,[3] Maxie M. Roessler*,[1,4]

Redox reactions and paramagnetic intermediates are ubiquitous in biological chemistry. We report a new method, protein film electrochemical electron paramagnetic resonance spectroscopy (PFE-EPR), that enables the direct and accurate potential control of proteins on the electrode surface for both electrochemical and EPR spectroscopic characterisation of their redox centres.

Electrochemistry and electron paramagnetic resonance (EPR) spectroscopy have found many applications in the chemical sciences.[1–3] The usefulness of combining these two techniques to access both detailed information on redox processes and structures of paramagnetic states in order to gain mechanistic understanding of chemical reactions is well-recognised with the first experiments dating back to the 1970s.[4] EPR spectroelectrochemical (SEC) studies so far fall broadly into two categories: (1) the in-situ detection of paramagnetic species in solution,[5,6] and (2) ex-situ electrogeneration followed by EPR measurements. In the latter, EPR measurements are often conducted using frozen solutions, especially when applied to biological samples that typically contain paramagnetic intermediates not being EPR-detectable at room temperature.

Most EPR SEC studies have been devoted to short-lived radicals in small molecules, and submicromolar concentrations of organic radicals have been detected with accurate potential control (i.e. in the absence of redox-active molecules termed 'mediators').[7] However, the detection of radical species in large protein complexes with direct and accurate potential control has thus far not been reported. Yet the plethora of redox reactions occurring in proteins and enzymes, many at metal centres, and the presence of numerous mechanistically-relevant paramagnetic intermediates, warrants the development of an EPR SEC method with precise potential control in macromolecules. Examples include redox-centres in many of the essential membrane proteins in photosynthesis and respiration, as well as hydrogenases (H_2 production and oxidation), nitrogenases (N_2 activation), to name but a few.

Direct electrochemical control of biomolecules for EPR spectroscopic investigations is currently challenged by their slow diffusion to the working electrode surface, and potentiometric titrations require mediators to determine reduction potentials of redox-active centres.[8] Such potentiometric titrations can only be carried out on steady-state radicals and are thus not suitable for detecting fleeting paramagnetic intermediates, for example those formed during enzyme catalysis. The primary difficulty in EPR SEC studies with proteins is slow diffusion, which can in principle be overcome by using protein film electrochemistry (PFE) that investigates the protein directly attached on the working electrode surface. This technique is thus not limited by mass transport of the redox-active species to the electrode and requires only picomolar sample concentrations, amongst other advantages discussed elsewhere.[9] PFE has already unravelled mechanistic details for numerous redox proteins, e.g. hydrogenases,[10] and has been successfully coupled with other spectroscopies.[11,12] To the best of our knowledge, the combination of PFE with EPR spectroscopy has not been previously reported.

Here, we demonstrate that the technical challenges of achieving direct (i.e. non-mediated), accurate potential control of biomolecules with sufficient sensitivity for EPR detection can be overcome by protein film-electrochemical EPR (PFE-EPR). To make our (protein) film electrochemical EPR method widely applicable, we constructed our cell in such a way that it is compatible with commercially-available EPR equipment (Fig. 1) and investigate the stable redox-active radical (4-amino-2,2,6,6-tetramethylpiperidine-1-oxyl, henceforth 4-amino TEMPO) and the enzyme Cu-Zn superoxide dismutase (henceforth SOD).

[1]School of Biological and Chemical Sciences and Materials Research Institute, Queen Mary University of London, Mile End Road, London E1 4NS, UK
[2]Department of Chemistry, NIS Centre and INSTM Reference Center, University of Turin, Turin, Via Giuria 7, 10125 Italy
[3]Department of Chemistry, University of Cambridge, Lensfield Road, Cambridge CB2 1EW, UK
[4]Department of Chemistry, Imperial College London, Molecular Sciences Research Hub, White City Campus, Wood Lane, London W12 0BZ, UK
E-mail: m.roessler@imperial.ac.uk
Electronic Supplementary Information (ESI) available: [details of any supplementary information available should be included here]. See DOI: 10.1039/x0xx00000x

Please do not adjust margins

We first designed, constructed and optimised the working electrode (WE), which is inserted into the EPR resonator (see ESI for details). A major hurdle in combining PFE with EPR spectroscopy is ensuring high sensitivity for EPR detection of the proteins in contact with the working electrode. PFE usually uses pyrolytic graphite 'edge' electrodes, but they give rise to large radical signals and are thus unsuitable for EPR spectroscopy. We turned to mesoporous indium-tin oxide (meso-ITO), which is known to be an excellent WE material, owing to good conductivity, hydrophilicity, easy functionalisation[13] and ability to bind proteins such as hydrogenase[14] and Photosystem II.[15]

Meso-ITO cylinders, prepared using commercially-available ITO nanoparticles (< 50 nm, see ESI), of ca. 1.3 mm diameter and 5 mm length were constructed around a coiled titanium wire and annealed at 300 °C in air. The cylindrical meso-ITO structure exhibited excellent structural integrity (see scanning electron microscopy image in Fig. 1 inset and Fig. S1 in ESI) and conductivity typical for a degenerate semiconductor (Tables S1 and S2 in ESI). Electrochemical measurements were conducted anaerobically, by immersing the meso-ITO cylinder into a 4 mm diameter borosilicate glass tube with the electrolyte solution as well as a reference (RE) and a counter electrode (CE) for cyclic voltammetry and potentiometry.

As a proof of concept, 4-amino TEMPO was covalently anchored to the three dimensional (3D) meso-ITO WE (Fig. 2 and Fig. S2 in ESI), exploiting the high affinity of ITO for phosphonate groups.[13] The cyclic voltammograms (Fig. 3A) reveal a single electrochemically reversible wave with a reduction potential of E_m = +0.874 ± 0.011 V vs standard hydrogen electrode (SHE), corresponding to the nitroxide/oxoammonium cation redox process of 4-amino TEMPO (see Fig. 2C and D), which is in excellent agreement with previous work.[16] The peak separation of the oxidative and reductive peaks is greater compared to the flat electrochemical cell equivalent (Fig. S3 in ESI), which can be attributed to significant resistance within the porous ITO network as well as the Ohmic drop in the electrolyte and internal electrical circuit resistance (Fig. 3C and ESI Table S1).[17] The surface-bound nature of 4-amino TEMPO is evident from the linear dependence of peak currents on scan rate (Fig. 3A inset), impedance measurements (Fig. 3B) and rotational correlation times derived from the EPR spectra (Fig. S4 and Table S3 in ESI).

Assuming quantitative electroactive coverage from covalent anchoring, the number of 4-amino TEMPO molecules in the electrochemical set-up was calculated to be equivalent to an 8.5 mM solution (2 nmol per mm^2 of meso-ITO, see ESI and Fig. S5). This estimate is in good agreement with the high sensitivity evident from room-temperature continuous-wave (CW) EPR spectroscopic measurements, showing that the number of 4-amino TEMPO molecules anchored onto the cylindrical meso-ITO electrode is equivalent to a 7.2 mM solution (ESI Fig. S4).

Having established high EPR sensitivity, we tested the control of the electrochemical potential for our method. Eight distinct meso-ITO 3D electrodes were prepared and poised to different potentials ranging from 1.22 V to 0.20 V vs SHE using the electrochemical set-up (Fig. 1). Although a stable current was reached in less than five minutes (Fig. 3C), which is amongst the shortest times achieved for small molecules[7] and to our knowledge constitutes a new benchmark for proteins in electrochemical EPR[18] (vide infra for experiments with SOD), the lack of instant equilibration is attributed to cracks and resistance in the 3D meso-ITO WE structure (Fig. S1 in ESI).

Samples were flash-frozen and the corresponding CW EPR spectra are shown in Figure 3D (inset). A new electrode was assembled for each SEC sample as the meso-ITO structure was found to be unstable to repeated freeze-thaw cycles. The shape of the EPR spectra is typical of nitroxide radicals measured at

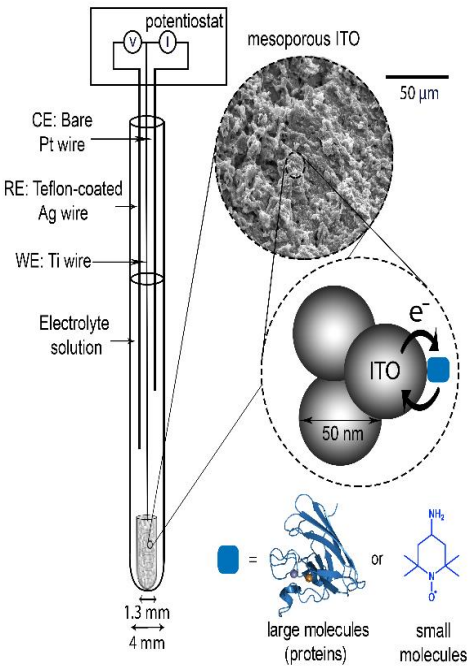


Figure 1. Schematic diagram of the PFE-EPR spectroelectrochemical cell. Borosilicate glass tube with meso-ITO WE (206 mm^2). Coiled Ti wire (O.D. 0.32 µm) maximises connection with meso-ITO structure. The pseudo-RE is Teflon-coated Ag wire (O.D. 0.125 µm) and CE is bare Pt wire (O.D. 0.125 µm). The electrolyte solution is phosphate-buffered saline (PBS) with 150 mM NaCl, adjusted to pH 7 or 8. Inset: scanning electron microscopy images of the meso-ITO electrode.

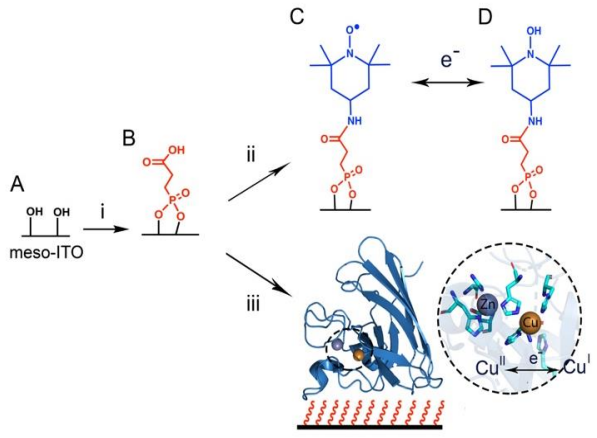


Figure 2. Schematic representation of the surface anchoring strategy for 4-amino TEMPO and SOD to meso-ITO. (A) Bare meso-ITO, (B) self-assembled monolayer, (C, D) oxidised and reduced 4-amino TEMPO. (i) Functionalisation using 3-phosphonopropanoic acid. (ii) Covalently anchorage of 4-amino TEMPO with coupling agents. (iii) Electrostatically anchored SOD. Inset: active site of SOD, with the redox-active Cu. A, B, C labels refer to the species characterised in Fig. 3B. See ESI for further details.

This journal is © The Royal Society of Chemistry 20xx

Please do not adjust margins

Please do not adjust margins

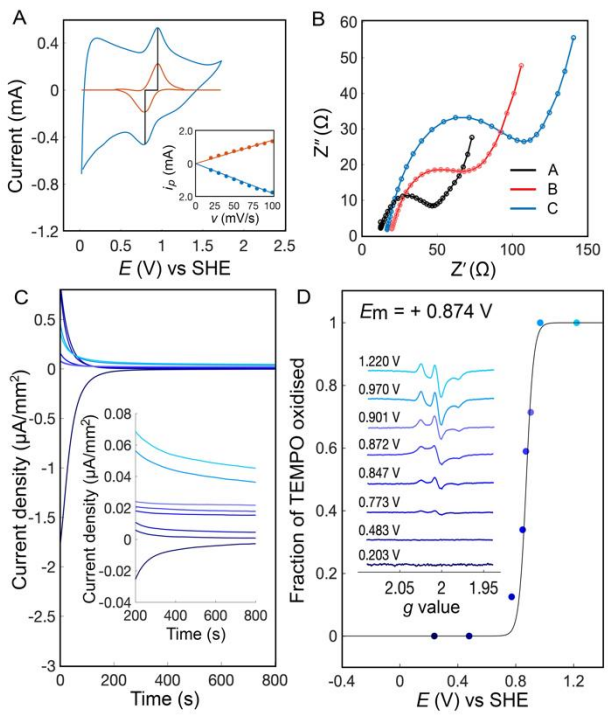


Figure 3. Electrochemical and EPR characterisation of 4-amino TEMPO in the PFE-EPR cell. (A) Cyclic voltammogram of 4-amino TEMPO in PBS, 0.15 M NaCl (pH 7.00), scan rate of 40 mV/s; inset: peak intensity against scan rate v. (B) Electrochemical impedance spectra to monitor functionalisation of meso-ITO, see Fig 2 for schematic diagram of the functionalisation steps. (C) Current response of potential-controlled potentiometry in the PFE-EPR cell; inset: zoom of 200 - 800 s timeframe. (D) Potentiometric titration: double integrals of individual EPR spectra (dots) and fit (solid line); inset: EPR spectra (100 K) of surface bound 4-amino TEMPO reduced to different potentials.

low temperatures.[19,20] The double integrals (i.e. areas) of individual EPR spectra were plotted as a function of potential and the resulting data points (* in Fig. 3D) fitted well onto the expected one-electron Nernst equation (solid line in Fig. 3D). Small deviations are attributed to the variability in the meso-ITO structure within each sample and the exact position of the EPR sample in the resonator, rather than any error in the applied potential. The reduction potential of +0.874 V vs SHE determined from the potentiometric titration (Fig. 3D) is in perfect agreement with that determined from cyclic voltammetry (Fig. 3A), demonstrating the accurate potential control of our film-electrochemical method.

To be able to carry out EPR measurements with a reasonable quality factor (Q = 1200 ± 100), only the bottom 1 mm³ of the borosilicate glass tube (Fig. 1) were inserted into the EPR resonator (for low-temperature measurements carried out in water, see ESI). This is perhaps unsurprising in light of the high-conductivity of the sample (primarily lowering Q), combined with the high dielectric constant of water. The resulting sensitivity (Fig. 3D inset) is excellent, considering that less than 1% of the fill-volume of the resonator is occupied by the paramagnetic sample.

To explore the suitability of our method for the investigation of proteins, we turned to Cu-Zn superoxide dismutase (SOD), a 16 kDa dimer. In principle any redox protein that can be attached in an electroactive configuration to ITO should be suitable for PFE-EPR. SOD was chosen because it is a well-characterised enzyme, with a clear electrochemical response resulting from the $Cu^{2+/+}$ redox couple,[21] that is EPR-active when oxidised (Cu^{2+}) and EPR-silent when reduced (Cu^{+}).[22] SOD from bovine erythrocytes was immobilised electrostatically onto the meso-ITO WE using self-assembled monolayers (Fig. 2 and ESI).[15,21]

The reduction potential obtained from cyclic voltammetry (Fig. 4A, see also ESI Fig. S6), carried out in the electrochemical set-up depicted in Fig. 1, resulted in a reduction potential E_m = +0.123 V vs SHE of the $Cu^{2+/+}$ redox process that agrees with previous work.[21] The linear relationship of peak current against scan rate (Fig. 4B) demonstrates the surface-bound nature of SOD. Peak currents remained unchanged after 100 scans at 20 mV/s (ESI Fig. S7), showing excellent stability of SOD on ITO.

To assess the quality of potential control for this sizeable protein, we conducted a potentiometric titration analogous to that described for 4-amino TEMPO, with selected resulting EPR spectra shown in Fig. 4C (for a full set of EPR spectra see ESI Fig. S8). As expected, the Cu^{2+} EPR signal decreases and ultimately vanishes with decreasing potential. The SOD anchored to the meso-ITO was determined to be equivalent to a 44 μM solution of SOD in buffer (12 pmol/mm² of ITO), as determined with UV-vis spectroscopy (see ESI and Fig. S3) explaining the notably good signal-to-noise ratio in the EPR spectra. With only approximately 1 mm³ of the meso-ITO bound SOD inserted into the EPR resonator, the high sensitivity is attributed to the large surface area available for protein immobilisation in the meso-ITO working electrode.

The resulting 'Nernst curve' for the $Cu^{2+/+}$ redox couple in SOD was obtained by plotting the intensity of $g_{x,y}$ transition as a function of the applied potential (Figure 4C). The reduction potential of E_m = +0.123 V vs SHE determined from fitting the one-electron Nernst equation (solid line) is in excellent agreement with the value obtained from cyclic voltammetry.

We have demonstrated the first successful direct combination of PFE with EPR spectroscopy, which provides

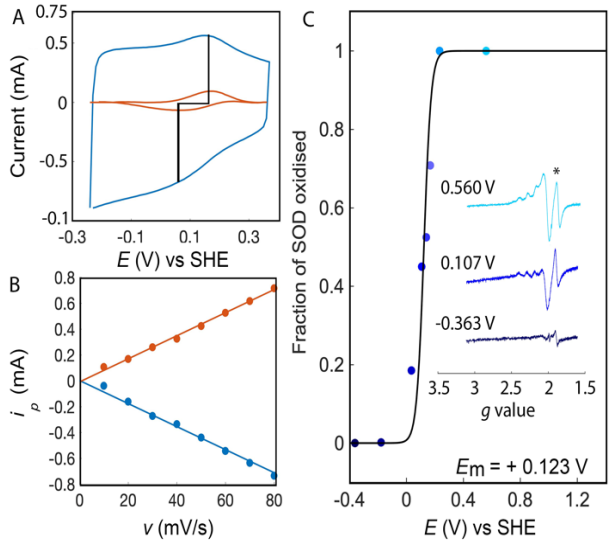


Figure 4. EPR SEC response of SOD in the PFE-EPR cell. (A) Cyclic voltammogram of SOD in PBS, 0.15 M NaCl (pH 8.02) at 60 mV/s. (B) Plot of peak intensity against scan rate. (C) Intensity of $g_{x,y}$ transition of Cu^{2+} in SOD (dots) and fit (solid line). Inset: CW EPR spectra (16 K) of surface bound SOD. * signal from meso-ITO electrode (see ESI Fig. S9).

Please do not adjust margins

Please do not adjust margins

exquisite potential control of a redox-active protein in the absence of any redox mediators for EPR spectroscopic investigations. The purpose of this PFE-EPR method is *not* to determine reduction potentials – for which classical EPR-monitored potentiometric titrations with mediators, such as the small-volume method we reported recently,[8] should suffice. Rather, the determination of the reduction potential of 4-amino TEMPO and SOD by cyclic voltammetry and by titration, and the goodness of the fit of the latter to the one-electron Nernst equation, was carried out to assess the accuracy of potential control.

In the future, we envisage that it will be possible to harness the full palette of advantages that stem from PFE, in particular the possibility to trap paramagnetic intermediates under precise electrochemical conditions during catalysis, to obtain structural information from EPR spectroscopy, ultimately including pulse methods to give detailed insight that is often not accessible with continuous-wave EPR alone.[3] To achieve this, a number of challenges will need to be overcome. "Wiring" *any* protein to the electrode in the right configuration can be a limitation of PFE.[23,24] Moreover, our working electrode material will need to be improved to enable instant potential control and to make it fully EPR-silent. Experiments with custom-made ITO nanoparticles are underway, as is the construction of inverse-opal ITO architecture[14] to accommodate larger protein complexes.

Our method falls between the two main categories of EPR-SEC experiments discussed above: Whilst not in-situ, the direct potential control of (some) in-situ methods is retained. Besides the key feature of attaching the redox-active molecule to a highly tuneable electrode material that enables astonishing sensitivity, the success of our method has relied on the use of frozen samples for EPR measurements – as typically required for metalloproteins with fast-relaxing metal centres – which tolerates the high dielectric constant of water in combination with the conductive working electrode. In contrast to conventional EPR experiments, only nanomoles of protein are required, making PFE-EPR highly attractive for investigating proteins that are difficult to obtain in large quantities, in addition to other advantages that stem from PFE, such as probing the effect of pH and inhibitors easily and reversibly.

In conclusion, we have presented a novel method that enables direct, accurate and fast potential control of redox centres, together with the EPR spectroscopic characterisation of paramagnetic intermediates, in any molecule irrespective of its size. Whilst our method is widely and generally applicable to any redox-active molecule, we believe that with further refinement it will be particularly useful in its application to proteins and enzymes undergoing catalysis. By harnessing information both on reactions (through PFE) and the nature and structure of steady-state and non-steady state paramagnetic intermediates (though EPR), PFE-EPR promises to lead to new mechanistic understanding of redox-based processes in biomolecules.

K.A. thanks the Materials Research Institute (QMUL) for a studentship and is grateful to the Centre for Advanced ESR (CAESR, University of Oxford) and SPIN-Lab (Imperial College) for EPR measurement time. This work was supported by the EPSRC (EP/L011972/1 to CAESR, EP/P030548/1 to SPIN-Lab, EP/L015978/1, EP/G037221/1 and nanoDTC to E.R.), a DTA studentship (to K.P.S.) and an ERC Consolidator Grant 'MatEnSAP' (682833 to E.R.).

Conflicts of interest

There are no conflicts to declare.

References

1 A. J. Bard and L. R. Faulkner, *Electrochemical Methods: Fundamentals and Applications*, John Wiley & Sons, 2nd edn., 2001.
2 V. Chechik, E. Carter and D. Murphy, *Electron paramagnetic resonance*, Oxford University Press, Oxford, 2016.
3 M. M. Roessler and E. Salvadori, *Chem. Soc. Rev.*, 2018, **47**, 2534–2553.
4 J. D. Wadhawan and R. G. Compton, in *Encyclopedia of Electrochemistry*, Wiley-VCH Verlag GmbH & Co. KGaA, 2007.
5 P. R. Murray and L. J. Yellowlees, in *Spectroelectrochemistry*, eds. W. Kaim and A. Klein, The Royal Society of Chemistry, 1st edn., 2008, pp. 207–231.
6 P. Rapta, E. Dmitrieva, A. A. Popov and L. Dunsch, in *Org. Electrochem.*, CRC Press, 5th edn., 2016, pp. 169–190.
7 M. A. Tamski, J. V Macpherson, P. R. Unwin and M. E. Newton, *Phys. Chem. Chem. Phys.*, 2015, **17**, 23438–47.
8 J. J. Wright, E. Salvadori, H. R. Bridges, J. Hirst and M. M. Roessler, *J. Inorg. Biochem.*, 2016, **162**, 201–206.
9 C. F. Blanford, *Chem. Commun.*, 2013, **49**, 11130.
10 F. A. Armstrong, R. M. Evans, S. V Hexter, B. J. Murphy, M. M. Roessler and P. Wulff, *Acc. Chem. Res.*, 2016, **49**, 884–892.
11 P. A. Ash and K. A. Vincent, *Chem. Commun.*, 2012, **48**, 1400–1409.
12 N. Kornienko, K. H. Ly, W. E. Robinson, N. Heidary, J. Z. Zhang and E. Reisner, *Acc. Chem. Res.*, DOI:10.1021/acs.accounts.9b00087.
13 M. Kato, T. Cardona, A. W. Rutherford and E. Reisner, *J. Am. Chem. Soc.*, 2013, **135**, 10610–10613.
14 D. Mersch, C.-Y. Lee, J. Z. Zhang, K. Brinkert, J. C. Fontecilla-Camps, A. W. Rutherford and E. Reisner, *J. Am. Chem. Soc.*, 2015, **137**, 8541–9.
15 X. Fang, K. P. Sokol, N. Heidary, T. A. Kandiel, J. Z. Zhang and E. Reisner, *Nano Lett.*, 2019, **19**, 1844–1850.
16 J. E. Baur, S. Wang and M. C. Brandt, *Anal. Chem.*, 1996, **68**, 3815–3821.
17 B. Reuillard, K. H. Ly, P. Hildebrandt, L. J. C. Jeuken, J. N. Butt and E. Reisner, *J. Am. Chem. Soc.*, 2017, **139**, 3324–3327.
18 P. R. Murray, D. Collison, S. Daff, N. Austin, R. Edge, B. W. Flynn, L. Jack, F. Leroux, E. J. L. McInnes, A. F. Murray, D. Sells, T. Stevenson, J. Wolowska and L. J. Yellowlees, *J. Magn. Reson.*, 2011, **213**, 206–9.
19 R. J. Usselman, I. Hill, D. J. Singel and C. F. Martino, *PLoS One*, 2014, **9**, e93065.
20 C. Tansakul, E. Lilie, E. D. Walter, F. Rivera, A. Wolcott, J. Z. Zhang, G. L. Millhauser and R. Braslau, *J. Phys. Chem. C*, 2010, **114**, 7793–7805.
21 Y. Tian, L. Mao, T. Okajima and T. Ohsaka, *Anal. Chem.*, 2004, **76**, 4162–4168.
22 K. M. Beem, D. C. Richardson and K. V Rajagopalan, *Biochemistry*, 1977, **16**, 1930–1936.
23 C. Léger and P. Bertrand, *Chem. Rev.*, 2008, **108**, 2379–2438.
24 N. D. J. Yates, M. A. Fascione and A. Parkin, *Chemistry*, 2018, **24**, 12164–12182.

This journal is © The Royal Society of Chemistry 20xx

Please do not adjust margins